https://doi.org/10.5194/essd-2022-217
Preprint. Discussion started: 8 September 2022

Open Access Earth System Science Data Discussions

Global soil moisture storage capacity at 0.5° resolution for geoscientific modelling

Kang Xie[1,2,3], Pan Liu[1,2,3] *, Qian Xia[1,2,3], Xiao Li[1,2,3], Weibo Liu[1,2,3], Xiaojing Zhang[1,2,3], Lei Cheng[1,2,3], Guoqing Wang[4], Jianyun Zhang[4]

[1]State Key Laboratory of Water Resources and Hydropower Engineering Science, Wuhan University, Wuhan 430072, China.
[2]Hubei Provincial Key Lab of Water System Science for Sponge City Construction, Wuhan University, Wuhan 430072, China.
[3]Research Institute for Water Security (RIWS), Wuhan University, Wuhan 430072, China.
[4]State Key Laboratory of Hydrology-Water Resources and Hydraulic Engineering, Nanjing Hydraulic Research Institute, Nanjing 210029, China.

Correspondence to: Pan Liu (liupan@whu.edu.cn)

Abstract. Soil moisture storage capacity (SMSC) links the atmosphere and terrestrial ecosystems, which is required as spatial parameters for geoscientific models. However, there are currently no available common datasets of the SMSC on a global scale, especially for hydrological models since conventional evapotranspiration-derived estimates cannot represent the extra storage capacity for the lateral flow and runoff generation. Here, we produce a dataset of the SMSC parameter for global hydrological models. Joint parameter calibration of three commonly used monthly water balance models provides the labels for a deep residual network. The global SMSC is constructed based on the deep residual network at 0.5° resolution by integrating 15 types of meteorological forcings, underlying surface properties, and runoff data. SMSC products are validated with the spatial distribution against root zone depth datasets and validated in the simulation efficiency on global grids and typical catchments from different climatic regions. We provide the global SMSC parameter dataset as a benchmark for geoscientific modelling by users.

1. Introduction

Soil moisture in the root zone layer is one of the vital hydrological variables in Earth system dynamics (Wang-Erlandsson et al., 2022). Soil moisture storage capacity (SMSC[L]) is defined as the total amount of water stored in the soil within the plant root zone, one of the essential parameters

https://doi.org/10.5194/essd-2022-217
Preprint. Discussion started: 8 September 2022

linking the atmosphere and terrestrial ecosystems in the hydrological components (Chen, 2014; Mccormick et al., 2021). The rooting depth of the plant cover determines the extent to which vegetation returns water into the atmosphere via plant transpiration (Kleidon, 2004). A deeper SMSC means a larger volume of water stored in the soil and, therefore, a larger reservoir of water available for crops to draw from. Additionally, SMSC determines the storage and outflow capacity of water and is one of the comprehensive parameters that affect the rainfall-runoff relationship. Therefore, the global parameterization of SMSC is necessary for geoscientific modelling. The SMSC has been widely applied in the hydrological models, such as Xinanjiang Model (Xie et al., 2020b; Zhao, 1992), Dynamic Water Balance Model (DWBM) (Wang et al., 2011; Zhang et al., 2008), Snowbelt-based Water Balance Model (SWBM) (Wang et al., 2014), and Time-variant Gain Model (TVGM) (Wang et al., 2009; Xia et al., 1997), etc. These hydrological models at different spatial and temporal scales have the same runoff generation structure, and SMSC becomes an essential parameter in the hydrological process (Bai et al., 2015; Jaiswal et al., 2020).

Broadly, previous studies have investigated conventional approaches to estimating the spatial distribution of the storage capacity in the root zone (Fan et al., 2017; Wang-Erlandsson et al., 2016; Yang et al., 2016). However, there is currently no consensus on the estimation of SMSC. Even with rooting depth measurements in situ from various field and laboratory observations, it is difficult to estimate the root zone storage capacity due to uncertainty in root density, hydrological activity, and horizontal spatial heterogeneity in soil data. The conventional calibration approach is only suitable for applications at the catchment scale, and therefore challenges remain with parameter equifinality. The conventional cumulative water deficit approach usually estimates soil plant-available water storage capacity from remote-sensing-based precipitation and evapotranspiration fluxes (Stocker et al., 2021). However, evapotranspiration-derived estimates of root-zone depth cannot represent the lateral flow and runoff generation. Soil water is not only absorbed by vegetation from root soil and stems for evaporation but also retains more capacity for runoff generation and groundwater flow. Overall, to our knowledge, little attention has been paid to quantifying a common global SMSC parameter from the perspective of the rainfall-runoff relationship in hydrological and land surface models (Beck et al., 2015a; Beck et al., 2015b; Nijssen et al., 2001). Conventionally estimated SMSC datasets are difficult

https://doi.org/10.5194/essd-2022-217
Preprint. Discussion started: 8 September 2022

to obtain the advantage of the model performance in global hydrological models.

Intense temporal unevenness and spatial heterogeneity have led to myriad problems in the parameterization solution (Ming et al., 2017; Blschl et al., 2019). Most global hydrological models are not calibrated or use prior knowledge to adjust SMSC parameters at large catchment scales since calibrations become computationally intensive under large amounts of data and uncertainty from basin characteristics (Wang et al., 2021). Essential parameters are even calibrated uniformly to subbasins over the entire watershed or only against regional data. During the last decade, much work has been done on the parameters and spatiotemporal boundaries of models (Chen, 2014; Imhoff et al., 2020; Samaniego et al., 2010; Vinogradov et al., 2011). The results demonstrated that the spatial distributions of regionalized parameters matched well with the climate and physiographic properties (Gentine et al., 2012). Samaniego et al. (2010) proposed a multiscale parameter regionalization (MPR) technique by a nonlinear transfer function and achieved the parameter transferability across the ungauged areas. Tsai et al. (2021) proposed a differentiable parameter learning (DPL) framework that efficiently learns a global mapping between dynamic inputs and hydrological parameters, and a deep learning model is trained to generate the generic parameters. Hence, many approaches have demonstrated the necessity and the feasibility of considering spatial heterogeneity in the hydrological process in quantifying a common global SMSC parameter dataset.

This study seeks the global construction of the common SMSC parameter while accepting the existing differences among hydrological models. The structure of the construction method is shown in **Figure 1**. Specifically, the spatial distribution of SMSC parameters is obtained by the Shuffled Complex Evolution (SCE-UA) algorithm for the joint calibration against an observation-based global gridded runoff (GRUN) dataset. A deep residual network (ResNet) is used to learn the relationship between the input factors and the regression SMSC parameters to consider spatial heterogeneity. The results of the joint calibration provide the labels for the training of ResNet. Finally, the SMSC parameter dataset is spatially constructed based on the pre-trained ResNet on the grid-scale to fill in data empty areas where SMSC parameters are not available by the calibration approach. The global runoff database center (GRDC) station streamflow data validates the global SMSC parameter dataset. Solving the problem of common parameter datasets can help improve the simulation accuracy of global

https://doi.org/10.5194/essd-2022-217
Preprint. Discussion started: 8 September 2022

hydrological models and help explore the physical meaning of model parameters associated with surface heterogeneity. The global modeling community would benefit significantly from more common parameter datasets.

[Please insert **Figure 1** here]

2. Data

Meteorological forcings and underlying surface properties affect the soil water storage capacity from hydrological processes, soil structure, and plant root zone. The model inputs include 15 variables such as global meteorological data, soil and vegetation data, topographical data, and streamflow characteristics. **Table 1** provides the data sources used in the study.

[Please insert **Table 1** here]

There are two different types of inputs, a continuous value input represented by precipitation and elevation and a categorical input represented by soil type and vegetation type. The model inputs are standardized. Time series values of meteorological data are used as inputs of the hydrological model. The multi-year averages of meteorological data are used as the spatial inputs to the deep learning model. Monthly measurements cover the year from 1902 to 2014 in the global grids. The data for the first year is used for warm-up, 80 years for calibration, and the remaining 30 years for validation.

3. Methods

3.1 Gridded-based monthly water balance models

Water balance models are one of the attractive models among the available hydrological simulation techniques, offering flexibility and comprehensibility (Abdollahi et al., 2017; Rodríguez-Huerta et al., 2020; Schaake et al., 1996). Water balance models can estimate daily, monthly, and annual hydrological variables and processes by considering soil moisture. The advantages of simple structure, fewer parameters, and fewer data requirements positively affect calibration and regionalization.

Monthly water balance models simulate and predict the monthly runoff under different climatic conditions (Do et al., 2020; Gui et al., 2019; Xiong et al., 2019). Monthly runoff processes differ from

https://doi.org/10.5194/essd-2022-217
Preprint. Discussion started: 8 September 2022

daily runoff because they generalize the stochastic uncertainty over a short time scale. Therefore, there is no need to distinguish runoff yield and route in monthly water balance models, leading to simple structures and straightforward applications (Zhang et al., 2018). Most monthly water balance models have the concept of a water tank model (Bai et al., 2015; Singh and Woolhiser, 2002). This study selects three monthly water balance models for the SMSC parameter.

(1) Dynamic Water Balance Model (DWBM)

The dynamic water balance model used in this study is the Budyko framework model by Wang et al. (2011) and Zhang et al. (2008). The mean annual water balance can be modeled using the method of Budyko (1958) by only considering dominant controls on evaporation. Fu (1981) developed the following relationships for estimating mean annual evaporation:

$$\frac{E}{P} = 1 + \frac{E_0}{P} - \left[1 + \left(\frac{E_0}{P}\right)^{\omega}\right]^{1/\omega} \quad (1)$$

where E is the mean annual actual evaporation, E_0 is the potential evaporation, and ω is a model parameter with the range of (1,∞). The catchment is conceptualized as a system of two storages: root zone storage and groundwater storage. Direct runoff can be calculated by rainfall $P(t)$ in time step t deducting catchment rainfall retention $X(t)$

$$Q_d(t) = P(t) - P(t)F\left(\frac{X_0(t)}{P(t)}, \alpha_1\right) \quad (2)$$

where $F()$ is Fu's curve - Eq. (1), α_1 is retention efficiency, i.e., a larger α_1 the value will result in more rainfall retention and less direct runoff. Evaporation E(t) can be calculated as

$$E(t) = W(t)F\left(\frac{E_0(t)}{W(t)}, \alpha_2\right) \quad (3)$$

where $W(t)$ is water availability, and α_2 is a model parameter representing evaporation efficiency. The soil water storage can now be calculated as:

$$S(t) = W(t)F\left(\frac{E_0(t)+SMSC}{W(t)}, \alpha_2\right) - E(t) \quad (4)$$

where $SMSC$ is the soil moisture storage capacity. Finally, the soil water storage is treated as a linear reservoir so that the groundwater balance and baseflow can be modeled as:

$$Q_g(t) = K_g S(t-1) \quad (5)$$

https://doi.org/10.5194/essd-2022-217
Preprint. Discussion started: 8 September 2022

$$G(t) = (1 - K_g)S(t-1) + R(t) \quad (6)$$

where $S(t)$ is groundwater storage, and K_g is a constant model parameter.

(2) Snowbelt-based Water Balance Model (SWBM)

The snowbelt-based water balance model used in this study is the Yellow river water balance model by Wang et al. (2014). According to the influencing factors of surface runoff yield, the calculation formula of surface runoff is put forward by generalizing the two runoff generation mechanisms:

$$Q_d(t) = K_s \frac{S(t)}{SMSC} P(t) \quad (7)$$

where $Q_d(t)$ is the direct surface runoff, $S(t)$ is the soil moisture, and $SMSC$ is the maximum soil moisture storage capacity, and K_s is the coefficient of surface runoff. It is assumed that the underground runoff is a linear reservoir discharge. The underground runoff is calculated as follows:

$$Q_g(t) = K_g S(t-1) \quad (8)$$

where $Q_g(t)$ is the underground runoff, and K_g is the coefficient of the underground runoff. The evaporation capacity of the basin is equal to that of the water surface. The calculation of long-term evaporation of the basin is based on the calculation model of soil evaporation as follows:

$$E(t) = E_m \frac{S(t-1)}{SMSC} \quad (9)$$

where $E(t)$ is the actual evaporation, E_m denotes the evaporation capacity of the basin and is calculated according to the meteorological data.

(3) Time-variant Gain Model (TVGM)

The relationship between rainfall and runoff is nonlinear. To grasp its nonlinear nature from system theory, Xia et al. (1997) and Wang et al. (2009) proposed the time-variant gain model (TVGM) model. The TVGM model can describe the nonlinear relationship between input and output of the hydrological cycle system by introducing a time-varying gain factor. The direct surface runoff generated by the catchment can be expressed as:

$$Q_d(t) = g_1 \left(\frac{S(t)}{SMSC}\right)^{g_2} P(t) \quad (10)$$

https://doi.org/10.5194/essd-2022-217
Preprint. Discussion started: 8 September 2022


Open Access Earth System Science Data Discussions

where $S(t)$ is the soil humidity at the beginning of the period, SC is the saturated soil humidity, P is rainfall, g_1 and g_2 are the related parameters of the time-varying gain factor, where g_1 is the runoff coefficient after soil saturation, g_2 is the soil moisture influence coefficient. Soil moisture flow is calculated as follows:

$$Q_g(t) = K_r[S(t-1) + S(t)]/2 \tag{11}$$

where K_r is the coefficient of soil moisture outflow. The actual evaporation is based on the rainfall-evaporation model considering soil moisture as follows:

$$E(t) = PET(t)\left(\frac{S(t)}{SMSC}\right)^{\gamma} \tag{12}$$

where γ is the weight coefficient of evaporation.

3.2 Parameter calibration strategy

In principle, parameters in the hydrological model are constructed based on the interpretation of the measured response in the catchment. However, for those parameters for which no measured values are available, the initial values of the parameters can first be determined empirically or by referring to previous results. Then the parameters are optimized according to the specific objectives against simulation results. Processes at different scales interact and influence each other, leading to the complexity of parameter calibration. The calibration will result in the spatially discontinuous parameter in each basin. The calibration aims to consider the spatial interactions of the parameters but often pursues the simulation accuracy too much since inputs are homogenized across catchments. Different areas make it difficult for the parameters to converge to spatially continuous values. Therefore, the parameters are calibrated on a spatial grid of the same area in this study. Research has shown that calibration on the global grids can significantly reduce parameter discontinuities compared to calibration on individual catchments (Xie et al., 2020a). The conceptual parameters in three monthly water balance models (**Table 2**) are calibrated against the agreement between simulated and observed hydrographs until the optimal value is obtained.

[Please insert **Table 2** here]

Two parameter calibration strategies are listed below, and the joint calibration strategy is

https://doi.org/10.5194/essd-2022-217
Preprint. Discussion started: 8 September 2022

considered in this study.

Individual calibration strategy: Each model is calibrated separately across global grids. The purpose is to find the similarities and differences in the SMSC parameter distribution of three different model structures. The gridded runoff depth data is used as observations for the calibration. The gridded global monthly runoff time series are obtained from the GRUN dataset on a 0.5 degrees grid covering 1902 to 2014 (Ghiggi et al., 2019a; Ghiggi et al., 2019b; Ibarra et al., 2020). The parameters calibrated in the catchment are used as the initial values on catchment grids.

Joint calibration strategy: This procedure will calibrate all parameters of three models in a joint calibration, and the SMSC parameters in each model are equal. The physical meaning of the parameters can only be expressed in terms of the same values. There should be a value between the optimal values of multiple models. This value has a physical meaning in terms of spatial continuity and can be commonly considered for each model.

The SCE-UA algorithm, one of the common global optimization methods, is used for the parameter calibration of monthly water balance models (Duan et al., 1994). The objective function is selected as the least-squares method, i.e., Mean Square Error (MSE). The Kling-Gupta Efficiency (KGE) is used to quantify the performance of the model simulations, which is a model evaluation criterion that can be decomposed into the contribution of mean, variance, and correlation to model performance (Gupta et al., 2009). KGE is calculated as follows:

$$\mathrm{KGE} = 1 - \sqrt{(r-1)^2 + (\mu_{sim}/\mu_{obs} - 1)^2 + (\sigma_{sim}/\sigma_{obs} - 1)^2} \quad (13)$$

where r is the Pearson Correlation Coefficient, μ and σ are the mean and common deviation of the variables. KGE value ranges from $-\infty$ to 1, with a value closer to 1 indicating a better simulation performance.

3.3 Deep residual network

Although the parameters obtained by the calibration at grid scale are accurate and have good spatial continuity, it is still challenging to obtain parameters on many unsuitable grids due to the limitations of the hydrological model in the ungauged area. It remains a daunting challenge to mine the

https://doi.org/10.5194/essd-2022-217
Preprint. Discussion started: 8 September 2022

hidden information from a large amount of data because of the inherent physical variability in complex physical mechanisms (Clark et al., 2016; Zhang and Liu, 2021). Driven by the increasingly powerful performance of computers and big data, statistical and non-inferential deep learning methods enable machines to have the same ability to analyze and learn as human beings (Kadow et al., 2020; Karpatne et al., 2018; Sit et al., 2020). Recent case studies have revealed that deep learning networks have succeeded in geoscience fields (Karpatne et al., 2018; Xie et al., 2021). It has been widely used for spatial missing data (Kadow et al., 2020), spatial downscaling (Jiang et al., 2021; Nearing et al., 2021), rainfall simulation improvement (Liu et al., 2020), and spatial phenomena prediction (Pan et al., 2019). Convolutional neural networks (CNNs) can automatically learn features from massive data and generalize the results to unknown domains of the same type (Shin et al., 2016). The convolution and pooling layers in CNNs only work on a local neighborhood, which helps to capture local geometric features and spatial patterns and extract larger-scale representations in deeper layers (Shen, 2018). The filters are shared when calculating the neurons of the same depth slice, which reduces the number of parameters and makes them easier to train.

A deep residual network, one of the specific types of CNN method, can automatically learn features from large-scale data and generalize the results to anonymous data of the same type (He et al., 2016). However, CNN has reached saturation accuracy when the number of layers deepens, called degradation. The network's performance deteriorates, and it is challenging to train shallow networks by backpropagation because the gradient dissipation is more severe. ResNet solves this problem by making it easier for gradients to flow into external networks. The structure of ResNet adds the residual mapping and the identity mapping through shortcut connections. If the network has reached the optimal level and continues to deepen, the residual mapping will be pushed to zero, leaving only identity mapping. Theoretically, the network has been in the optimal state, and the network performance does not decrease with increasing depth. Finally, the gradient vanishing can be avoided, and the network can be deepened. ResNet provides a new approach to learning SMSC parameters using more information from similar grids (Zhuo and Tan, 2021).

CNN local connection means that each neuron is connected to only one region of the input neuron, and the filters used by CNN to compute neurons of the same depth slice are shared. These

https://doi.org/10.5194/essd-2022-217
Preprint. Discussion started: 8 September 2022

characteristics are similar to the hydrological parameters and the spatial characteristics of the input data. From the conventional statistic method to the deep paradigm, ResNet has the following three outstanding advantages against conventional statistic methods.

(1) ResNet is provided with the more vital generalization ability. Conventional statistic methods cannot explore the complex inner connections of the soil water process, while ResNet avoids directly interpreting the physical meaning of the parameters firstly.

(2) More input variables are used in ResNet. Conventional root depth calculations use only precipitation and evaporation, while both meteorological forcings, underlying surface properties, and runoff data are considered in ResNet.

(3) ResNet has faster speed and higher performance. Conventional statistic methods cannot learn complex interactions and are slow to compute. However, parallel computing is used in ResNet, and the network is complex but much faster. The model is run on a GPU (Nvidia Tesla V100 16GB) cluster and takes 758 microseconds per step, about one hour on all global 0.5-degree grids.

3.4 Training and testing

The SMSC parameters on the global grids obtained by the calibration algorithm are taken as the target labels of the model. On grids with KGE greater than 0, SMSC parameters can be obtained by calibrating the hydrological model. However, the hydrological model cannot be built in some areas where the model is not applicable, such as highly arid areas. Areas with KGE less than 0 are masked. On grids with KGE greater than zero, the samples are divided into the training set and test set according to the ratio of 7:3.

Table 3 shows the learning performance of the training and test sets for different image windows. The results show that the recognition network is poor if the image window is too small. The effect of 10 × 10 image windows is better than that of 5 × 5 grid windows, and the effect of 100 surrounding grids on the center grid can be considered for 10 × 10 windows. The Correlation coefficient (R^2) of the test set increases from 0.59 to 0.76. The computational burden from the increase in image windows is no longer as cost-effective as the increase in inefficiency.

[Please insert **Table 3** here]

https://doi.org/10.5194/essd-2022-217
Preprint. Discussion started: 8 September 2022

3.5 Permutation importance

The deep learning network is often considered a black-box model, and here interpretation techniques are used in order to better understand the underlying relationships tapped by deep learning. Permutation feature importance is a model inspection technique widely used for deep learning networks (Altmann et al., 2010). For a fitted predictive model, permutation importance can compute the reference score of the model on the dataset. The importance i_j for each feature f_j defined as:

$$i_j = s - \frac{1}{K}\sum_{k=1}^{K} s_{k,j} \quad (14)$$

where s is the reference score of the model, for instance, the accuracy for a classifier or the correlation coefficient (R^2) for a regressor, k is each repetition in input factors.

4. Evaluation of the global soil moisture storage capacity

4.1 Comparison of the spatial distribution with other parameter datasets

Figure 2a shows the SMSC values jointly calibrated by setting the SMSC parameters of the three models to be the same. The results show that combined objectives for the calibration of three models are relatively stricter, with only 45% of the grid KGE greater than zero, which is called the labeling area (the opposite corresponding to the constructing area). The SMSC parameters are larger in humid areas and smaller in arid areas. The hydrological model is no longer applicable outside the labeling area, such as semi-arid and cold regions. **Figure 2**c shows the probability density distribution of SMSC parameters calibrated in the labeling area. It can be found that the distribution of the jointly calibrated SMSC parameters is consistent with the distribution of the individually calibrated SMSC parameters. **Figure 2**b shows the spatial distribution of the global SMSC parameters both in the labeling area and the constructing area. The constructed SMSC is also larger in humid regions and smaller in arid regions. The parameters are larger in high-altitude regions. **Figure 2**d and **Figure 2**f show the variation of global SMSC with latitude and longitude. The results show that the global SMSC is largest at the equator and decreases toward the poles. **Figure 2**e shows the probability density function of the global SMSC with a double-peak distribution. The first peak corresponds to the arid region, and the second peak corresponds to the humid region.

https://doi.org/10.5194/essd-2022-217
Preprint. Discussion started: 8 September 2022


Open Access Earth System Science Data Discussions

[Please insert **Figure 2** here]

We compared the spatial distribution of global SMSC with other parameter datasets. **Figure 3** shows estimations of global root zone parameters from previous studies and compares them to global SMSC. Root zone storage capacity at 0.5° resolution ($SR\_CRU_{Wang\text{-}Erlandsson}$, **Figure 3**a) is estimated by computing the maximum moisture deficit with independent energy balance equations by satellite-based evaporation from Wang-Erlandsson et al. (2016). Rooting depth at 1.0° resolution (SR_{Schenk}, **Figure 3**c) estimates the rooting depth that contains 95% of all roots from Schenk et al. (2009). By comparing these datasets with SMSC, we can see both agreements and significant differences. The purpose is the geographic comparison to other soil moisture storage capacity estimates. These comparisons are expected to find differences in the spatial distribution between root depth and soil moisture storage capacity. All datasets show a relatively similar spatial distribution, decreasing from the equator to the poles. All datasets have smaller values in the tropical rainforest region near the equator than our SMSC product. SR_{Schenk} tends to overestimate SMSC parameters in the Sahara Desert, Arabian Desert, and Western Australian Desert. ET-derived estimated water storage capacity might be relatively small in some areas. **Figure 3**b shows that the roots of vegetation ($SR\_CRU_{Wang\text{-}Erlandsson}$) may not be so deep, especially in the humid region of the equatorial, but our proposed SMSC data is deeper in the humid region. The findings indicate that ET-derived estimates of root-zone depth are unable to represent the lateral flow and runoff generation. Soil water is not only absorbed by vegetation from root soil and stems for evaporation but also retains more capacity for runoff generation and groundwater flow.

[Please insert **Figure 3** here]

4.2 Model performance of runoff depth in global grids

We tested runoff depth simulations of the global SMSC dataset on global grids. Gridded-based monthly water balance models are established on each 0.5 ° and 0.5 ° grid over the global terrestrial land. The SMSC parameters in these models adopt the proposed global SMSC dataset, while other parameters are recalibrated. The model parameter SMSC among the three monthly water balance models is the same in the proposed dataset constructed by CCN. This parameter is no longer recalibrated in further modeling. The inputs are monthly precipitation and evaporation for each grid. Monthly runoff depths of GRUN on this grid are used as the observations for model evaluation. **Figure**

https://doi.org/10.5194/essd-2022-217
Preprint. Discussion started: 8 September 2022

4a-c presents the distribution of simulation accuracy for three water balance models on the global grids. The models perform well in the humid region, semi-humid region, and most of the semi-arid region. The KGE performance of the models is significantly better in the humid region than in the semi-humid region and most of the semi-arid region. **Figure 4**d shows the KGE probability density distributions of three models. The results demonstrate that the TVGM model performs the best, with 20% of the grids having KGE values above 0.80 and 40% above 0.60. The results also indicate two distinct peaks in the KGE distribution of the SWBM model. The peak on the left represents the poor KGE of the SWBM model in the semi-humid and most semi-arid regions. **Figure 4**e shows the cumulative probability density distribution of KGE for three models on global grids, and **Figure 4**f shows the KGE box. What stands out in the figure is that the TVGM model has the best KGE, where the average KGE can reach 0.55, while the SWBM model is the worst.

As shown in **Figure 4**, the results indicate that TVGM and DWBM models perform better in the cold region. These three models do not take the temperature as the input, and therefore the snowbelt module is not considered. All three models do not perform very well in arid and semi-arid areas. The water balance model is challenging to simulate monthly runoff in arid areas because of the mismatch of the rainfall-runoff relationship.

[Please insert **Figure 4** here]

4.3 Model performance of streamflow in typical catchments

Station streamflow is used for the validation of global SMSC parameters. The GRDC dataset is a unique collection of river discharge data on a global scale (Peel et al., 2004; Peel et al., 2001). It contains daily and monthly river discharge data from over 10,000 stations worldwide. The selected validation basins require a basin area of more than 10,000km^2 and a monthly runoff record of more than five years from 1991 to 2010. Finally, data from 20 stations in different climatic regions are selected for validation. These 20 significant rivers are distributed in five different climate zones. **Table 4** lists the simulated KGE of three models in 20 typical catchments, and the average simulation accuracy is more than 0.65. **Figure 5** shows the dots of simulated streamflow versus observed streamflow during the validation periods.

[Please insert **Table 4** here]

https://doi.org/10.5194/essd-2022-217
Preprint. Discussion started: 8 September 2022

[Please insert **Figure 5** here]

The spatial patterns presented by the three models would be extraordinarily different if the three models were directly applied in the catchment according to the lumped model since different catchment areas influence them. Although this approach achieves good simulation accuracy, it does not consider the physical significance and spatially seamless alignment. However, the constructed global SMSC parameters have an excellent spatial continuity. The average values of the constructed SMSC parameter are calculated in 20 basins in different climatic regions as the recommended value of the parameters. **Figure 6** shows the simulation accuracy of $SR\_CRU_{Wang\text{-}Erlandsson}$ parameters in 20 basins compared with the SMSC parameters constructed in this study. The results show higher KGE performance of the constructed SMSC parameters in the three selected monthly water balance models in the 20 selected basins. Labels of the SMSC parameters are derived from the results of the model parameters, and more input information is considered in the construction. The purpose of the comparison is to evaluate the proposed dataset from the perspective of hydrological models. SMSC estimated from the model's perspective has achieved higher KGE performance and is more practical. The $CRU_{Wang\_Erlandsson}$ dataset is estimated using only two data types, precipitation, and evaporation, but it lacks model validation. Even if actual evaporation is also used in the calculation, the SMSC calculated by this method may not be able to simulate evaporation accurately because it lacks a model basis. On the contrary, our product utilizes a hydrological model, which can simultaneously simulate evaporation, runoff, and soil water content and achieve water balance.

[Please insert **Figure 6** here]

4.4 The sensitivity of input factors selection

Model input factors of the deep residual network include 15 variables affecting SMSC such as global meteorological data, soil and vegetation data, topographical data, and streamflow characteristics. These available factors, including meteorological forcings and underlying surface properties. Meteorology data include precipitation, potential evaporation, and near-surface temperature, which influence these processes such as evaporation, transpiration, and runoff in the water cycle. Soil data include soil thickness, root zone depth, soil type, and types of land use, which influence the soil structure. As the permutation importance estimate of **Figure 7** below shows, the most significant

https://doi.org/10.5194/essd-2022-217
Preprint. Discussion started: 8 September 2022

factors influencing the spatial construction of water storage capacity parameters in global grids are the precipitation and the type of land use. The precipitation, as the dominant factor in the spatial evolution of the SMSC parameter, explains more than 60% of the spatial distribution of SMSC. The precipitation and the type of land use directly influence the root zone depth and porosity of vegetation in different areas.

[Please insert **Figure 7** here]

5. Uncertainty of the data

However, there exists some uncertainty to this dataset. Meteorological data mainly include precipitation, temperature, and evaporation. Hydrological models are very sensitive to meteorological data, especially precipitation data. Firstly, data have intensively spatial and temporal variability. Most of the gird-based meteorological product comes from scattered observation sites, which cannot fully describe the spatial characteristics of features. Especially for large watersheds, the observation stations in the watershed cannot well represent the spatiotemporal changes, which may eventually affect the results of the model simulation. Secondly, there are also errors in the measurement data of the observation station, which leads to the uncertainty of the input data.

In addition to meteorological data as input data, spatial data such as digital elevation, land use data, soil type data, etc. are usually required. The accuracy of the spatial data to describe the characteristics of the watershed is the premise of the accurate simulation of the model. The resolution of the elevation, the accuracy of the land use type and the accuracy of the soil data type all have a certain impact on the simulation results. The level of resolution affects the extraction of parameters of the study watershed characteristics (slope, slope aspect, water and sediment migration direction, confluence network, watershed boundary, etc.), and ultimately affects the accuracy of the product.

The nonlinearity of the model structure and the correlation of parameters make the model solution space possible to have multiple local optimal solutions. The above effects all lead to large uncertainties in the process of watershed runoff simulation in the distributed hydrological model.

https://doi.org/10.5194/essd-2022-217
Preprint. Discussion started: 8 September 2022

6. Recommendations and limitations for the use of the data

This product is only limited by the current climatic conditions and ignores future changes. We estimated the SMSC based on the meteorological forcings, underlying surface properties, and runoff dataset over the calibration and validation period 1902-2014. Results may change when using data from different periods. Recent studies show that soil water storage capacity in the root zone changes with climate change and deforestation. The vegetation changes the ability to utilize subsoil moisture storage and tree cover to respond to arid climates. Additionally, the proposed dataset provides the global SMSC parameter dataset mainly for the water balance models at a monthly scale. At the current stage, it does not provide insights on quality simulations of low flow and high flow on a daily or hourly scale.

7. Code and data availability

A global terrestrial SMSC dataset with 0.5 ° spatial resolution is now available. The global construction map of SMSC in this study can be gathered from an open-access data server. All input factors and the global SMSC data are publicly available as NetCDF files or downloaded from smsc_data.zip at Zenodo (https://doi.org/10.5281/zenodo.5598405, Xie (2021)). Python codes are available to calculate the basin average SMSC value from grid values in any interested basin on a global scale. The Fortran codes for the parameter calibration of gridded-based global monthly water balance models are available at https://github.com/xiekangwhu/SMSC_monthly_water_balance_models. The Python codes of the deep residual network we developed for the global construction map of SMSC are available at https://github.com/xiekangwhu/SMSC_deep_residual_network.

8. Conclusions

In this paper, a new global SMSC dataset for global hydrological models is constructed by the deep residual network at 0.5° resolution by integrating 15 types of meteorological forcings, underlying surface properties, and runoff data. Compared with $SR\_CRU_{Wang\text{-}Erlandsson}$ and SR_{Schenk} dataset, the results show that the accuracy of the three gridded-based monthly water balance models from high to

https://doi.org/10.5194/essd-2022-217
Preprint. Discussion started: 8 September 2022

low is the proposed SMSC, $SR\_CRU_{Wang\text{-}Erlandsson}$ and SR_{Schenk}. Through the interpretation technique of the deep residual network, the most significant factors influencing water storage capacity parameters in global grids are precipitation and land use.

Author contribution

Kang Xie performed writing - original draft, conceptualization, methodology, and software.

Pan Liu performed writing - review and editing, conceptualization, and supervision.

Qian Xia performed the methodology of hydrological models.

Xiao Li performed data processing and coding.

Weibo Liu performed writing - review and editing.

Xiaojing Zhang performed the methodology of the parameter calibration strategy.

Lei Cheng performed writing - review and editing.

Guoqing Wang performed writing - review and editing.

Jianyun Zhang performed writing - review and editing, and supervision.

Competing interests

The authors declare that they have no competing interests.

Disclaimer

Publisher's note: Copernicus Publications remains neutral with regard to jurisdictional claims in published maps and institutional affiliations.

Acknowledgments

The authors appreciate the help from the Supercomputing Center of Wuhan University for providing the necessary guides to perform the numerical calculations of this study on the supercomputing system.

https://doi.org/10.5194/essd-2022-217
Preprint. Discussion started: 8 September 2022

Financial support

This study was supported by the Joint Funds of the National Natural Science Foundation of China (Grant No. U1865201), National Natural Science Foundation of China (Grant No. 51861125102), Innovation Team in Key Field of the Ministry of Science and Technology (Grant No. 2018RA4014), and the Young Scientists Fund of the National Natural Science Foundation of China (Grant No. 52109030).

References

Abdollahi, K., Bashir, I., Verbeiren, B., Harouna, M. R., Van Griensven, A., Huysmans, M., and Batelaan, O.: A distributed monthly water balance model: formulation and application on Black Volta Basin, Environmental Earth Sciences, 76, 198, 10.1007/s12665-017-6512-1, 2017.

Altmann, A., Toloşi, L., Sander, O., and Lengauer, T.: Permutation importance: a corrected feature importance measure, Bioinformatics, 26, 1340-1347, 2010.

Bai, P., Liu, X., Liang, K., and Liu, C.: Comparison of performance of twelve monthly water balance models in different climatic catchments of China, Journal of Hydrology, 529, 1030-1040, 10.1016/j.jhydrol.2015.09.015, 2015.

Beck, H., Roo, A. D., Dijk, A. V., Mcvicar, T., Miralles, D., Schellekens, J., Bruijnzeel, S., and Jeu, R. D.: Global-scale regionalization of hydrological model parameters using streamflow data from amany small catchments, Egu General Assembly Conference,

Beck, H. E., De Roo, A., and van Dijk, A. I.: Global maps of streamflow characteristics based on observations from several thousand catchments, Journal of Hydrometeorology, 16, 1478-1501, 10.1175/JHM-D-14-0155.1, 2015b.

Blschl, G., Bierkens, M., Chambel, A., Cudennec, C., and Zhang, Y.: Twenty-three unsolved problems in hydrology (UPH) – a community perspective, Hydrological Sciences Journal/Journal des Sciences Hydrologiques, 64, 1141-1158, 10.1080/02626667.2019.1620507, 2019.

Budyko, M.: The heat balance of the earth's surface, US Dept. of Commerce, Weather Bureau, Washington, DC, USA, 1958.

Chen, B.: Analysis of hydrologic systems at multiple spatial scales and its implications for aggregating hydrologic process, Dissertations & Theses Gradworks, 2014.

Clark, M. P., Schaefli, B., Schymanski, S. J., Samaniego, L., Luce, C. H., Jackson, B. M., Freer, J. E., Arnold, J. R., Moore, R. D., and Istanbulluoglu, E.: Improving the theoretical underpinnings of process-based hydrologic models, Water Resources Research, 52, 2350-2365, 10.1002/2015WR017910, 2016.

Do, H. X., Smith, J. P., Fry, L. M., and Gronewold, A. D.: Seventy-year long record of monthly water balance estimates for Earth's largest lake system, Scientific Data, 7, 1-12, 10.1038/s41597-020-00613-z,

https://doi.org/10.5194/essd-2022-217
Preprint. Discussion started: 8 September 2022

2020.

Duan, Q., Sorooshian, S., and Gupta, V. K.: Optimal use of the SCE-UA global optimization method for calibrating watershed models, Journal of hydrology, 158, 265-284, 10.1016/0022-1694(94)90057-4, 1994.

Fan, Y., Miguez-Macho, G., Jobbágy, E. G., Jackson, R. B., and Otero-Casal, C.: Hydrologic regulation of plant rooting depth, Proceedings of the National Academy of Sciences, 114, 10572-10577, 10.1073/pnas.1712381114, 2017.

Fu, B.: On the calculation of the evaporation from land surface, Sci. Atmos. Sin, 5, 23-31, 1981.

Gentine, P., Troy, T. J., Lintner, B. R., and Findell, K. L.: Scaling in Surface Hydrology: Progress and Challenges, Journal of Contemporary Water Research & Education, 147, 28-40, 10.1111/j.1936-704X.2012.03105.x, 2012.

Ghiggi, G., Humphrey, V., Seneviratne, S. I., and Gudmundsson, L.: GRUN: an observation-based global gridded runoff dataset from 1902 to 2014, Earth System Science Data, 11, 1655-1674, 10.5194/essd-11-1655-2019, 2019a.

Ghiggi, G., Seneviratne, S. I., Humphrey, V., and Gudmundsson, L.: GRUN: Global Runoff Reconstruction (GRUN_v1) [dataset], 2019b.

Gui, Z., Liu, P., Cheng, L., Guo, S., Wang, H., and Zhang, L.: Improving runoff prediction using remotely sensed actual evapotranspiration during rainless periods, Journal of Hydrologic Engineering, 24, 04019050, 10.1061/(ASCE)HE.1943-5584.0001856, 2019.

Gupta, H. V., Kling, H., Yilmaz, K. K., and Martinez, G. F.: Decomposition of the mean squared error and NSE performance criteria: Implications for improving hydrological modelling, Journal of hydrology, 377, 80-91, 2009.

He, K., Zhang, X., Ren, S., and Sun, J.: Deep residual learning for image recognition, Proceedings of the IEEE conference on computer vision and pattern recognition, 770-778,

Ibarra, D. E., David, C. P. C., and Tolentino, P. L. M.: Evaluation and bias correction of an observations-based global runoff dataset using historical streamflow observations from small tropical catchments in the Philippines, Hydrol. Earth Syst. Sci. Discuss., 10.5194/hess-2020-26, 2020.

Imhoff, R. O., Vanverseveld, W. J., Vanosnabrugge, B., and Weerts, A. H.: Scaling Point - Scale (Pedo)transfer Functions to Seamless Large - Domain Parameter Estimates for High - Resolution Distributed Hydrologic Modeling: An Example for the Rhine River, Water Resources Research, 56, 10.1029/2019WR026807, 2020.

Jaiswal, R., Ali, S., and Bharti, B.: Comparative evaluation of conceptual and physical rainfall–runoff models, Applied water science, 10, 1-14, 2020.

Jiang, Y., Yang, K., Shao, C., Zhou, X., Zhao, L., Chen, Y., and Wu, H.: A downscaling approach for constructing high-resolution precipitation dataset over the Tibetan Plateau from ERA5 reanalysis, Atmospheric Research, 256, 105574, 10.1016/j.atmosres.2021.105574, 2021.

Kadow, C., Hall, D. M., and Ulbrich, U.: Artificial intelligence reconstructs missing climate information, Nature Geoscience, 10.1038/s41561-020-0582-5, 2020.

https://doi.org/10.5194/essd-2022-217
Preprint. Discussion started: 8 September 2022

Karpatne, A., Ebert-Uphoff, I., Ravela, S., Babaie, H. A., and Kumar, V.: Machine learning for the geosciences: Challenges and opportunities, IEEE Transactions on Knowledge and Data Engineering, 31, 1544-1554, 10.1109/TKDE.2018.2861006, 2018.

Kleidon, A.: Global datasets of rooting zone depth inferred from inverse methods, Journal of Climate, 17, 2714-2722, 10.1175/1520-0442(2004)017<2714:GDORZD>2.0.CO;2, 2004.

Liu, Y., Jing, W., Wang, Q., and Xia, X.: Generating high-resolution daily soil moisture by using spatial downscaling techniques: A comparison of six machine learning algorithms, Advances in Water Resources, 141, 103601, 10.1016/j.advwatres.2020.103601, 2020.

McCormick, E. L., Dralle, D. N., Hahm, W. J., Tune, A. K., Schmidt, L. M., Chadwick, K. D., and Rempe, D. M.: Widespread woody plant use of water stored in bedrock, Nature, 597, 225-229, 10.1038/s41586-021-03761-3, 2021.

Ming, B., Liu, P., Guo, S., Zhang, X., Feng, M., and Wang, X.: Optimizing utility-scale photovoltaic power generation for integration into a hydropower reservoir by incorporating long-and short-term operational decisions, Applied Energy, 204, 432-445, 10.1016/j.apenergy.2017.07.046, 2017.

Nearing, G. S., Kratzert, F., Sampson, A. K., Pelissier, C. S., Klotz, D., Frame, J. M., Prieto, C., and Gupta, H. V.: What role does hydrological science play in the age of machine learning?, Water Resources Research, 57, e2020WR028091, 10.1029/2020WR028091, 2021.

Nijssen, B., Lettenmaier, D. P., Lohmann, D., and Wood, E. F.: Predicting the Discharge of Global Rivers, Journal of Climate, 14, 3307-3323, 10.1175/1520-0442(2001)014<3307:PTDOGR>2.0.CO;2, 2001.

Pan, B., Hsu, K., AghaKouchak, A., and Sorooshian, S.: Improving precipitation estimation using convolutional neural network, Water Resources Research, 55, 2301-2321, 10.1029/2018WR024090, 2019.

Peel, M. C., AMcMahon, T., and LFinlayson, B.: Continental differences in the variability of annual runoff-update and reassessment, Journal of Hydrology, 295, 185-197, 10.1016/j.jhydrol.2004.03.004, 2004.

Peel, M. C., McMahon, T. A., Finlayson, B. L., and Watson, F. G.: Identification and explanation of continental differences in the variability of annual runoff, Journal of Hydrology, 250, 224-240, 10.1016/S0022-1694(01)00438-3, 2001.

Rodríguez-Huerta, E., Rosas-Casals, M., and Hernández-Terrones, L. M.: A water balance model to estimate climate change impact on groundwater recharge in Yucatan Peninsula, Mexico, Hydrological Sciences Journal, 65, 470-486, 10.1080/02626667.2019.1702989, 2020.

Samaniego, L., Kumar, R., and Attinger, S.: Multiscale parameter regionalization of a grid-based hydrologic model at the mesoscale, Water Resources Research, 10.1029/2008WR007327, 2010.

Schaake, J. C., Koren, V. I., Duan, Q. Y., Mitchell, K., and Chen, F.: Simple water balance model for estimating runoff at different spatial and temporal scales, Journal of Geophysical Research: Atmospheres, 101, 7461-7475, 10.1029/95JD02892, 1996.

Schenk, H., Jackson, R., HALL, F., COLLATZ, G., MEESON, B., LOS, S., BROWN DE COLSTOUN,

https://doi.org/10.5194/essd-2022-217
Preprint. Discussion started: 8 September 2022

E., and LANDIS, D.: Islscp ii ecosystem rooting depths, ORNL DAAC, 2009.

Shen, C.: A transdisciplinary review of deep learning research and its relevance for water resources scientists, Water Resources Research, 54, 8558-8593, 10.1029/2018WR022643, 2018.

Shin, H.-C., Roth, H. R., Gao, M., Lu, L., Xu, Z., Nogues, I., Yao, J., Mollura, D., and Summers, R. M.: Deep convolutional neural networks for computer-aided detection: CNN architectures, dataset characteristics and transfer learning, IEEE transactions on medical imaging, 35, 1285-1298, 10.1109/TMI.2016.2528162, 2016.

Singh, V. P. and Woolhiser, D. A.: Mathematical modeling of watershed hydrology, Journal of hydrologic engineering, 7, 270-292, 10.1061/(ASCE)1084-0699(2002)7:4(270), 2002.

Sit, M., Demiray, B. Z., Xiang, Z., Ewing, G. J., Sermet, Y., and Demir, I.: A Comprehensive Review of Deep Learning Applications in Hydrology and Water Resources, Water Science and Technology, 82, 10.2166/wst.2020.369, 2020.

Stocker, B., Tumber-Dávila, S. J., Konings, A. G., Anderson, M. B., Hain, C., and Jackson, R. B.: Global distribution of the rooting zone water storage capacity reflects plant adaptation to the environment, 10.3929/ethz-b-000507551, 2021.

Tsai, W.-P., Feng, D., Pan, M., Beck, H., Lawson, K., Yang, Y., Liu, J., and Shen, C.: From calibration to parameter learning: Harnessing the scaling effects of big data in geoscientific modeling, Nature communications, 12, 1-13, 2021.

Vinogradov, Y. B., Semenova, O. M., and Vinogradova, T. A.: An approach to the scaling problem in hydrological modelling: the deterministic modelling hydrological system, Hydrological Processes, 25, 1055-1073, 10.1002/hyp.7901, 2011.

Wang-Erlandsson, L., Bastiaanssen, W. G., Gao, H., Jägermeyr, J., Senay, G. B., Van Dijk, A. I., Guerschman, J. P., Keys, P. W., Gordon, L. J., and Savenije, H. H.: Global root zone storage capacity from satellite-based evaporation, Hydrology and Earth System Sciences, 20, 1459-1481, 10.5194/hess-20-1459-2016, 2016.

Wang-Erlandsson, L., Tobian, A., van der Ent, R. J., Fetzer, I., te Wierik, S., Porkka, M., Staal, A., Jaramillo, F., Dahlmann, H., and Singh, C.: A planetary boundary for green water, Nature Reviews Earth & Environment, 1-13, 2022.

Wang, G., Xia, J., and Chen, J.: Quantification of effects of climate variations and human activities on runoff by a monthly water balance model: A case study of the Chaobai River basin in northern China, Water resources research, 45, 10.1029/2007WR006768, 2009.

Wang, G., Zhang, J., Jin, J., Liu, Y., He, R., Bao, Z., Liu, C., and Li, Y.: Regional calibration of a water balance model for estimating stream flow in ungauged areas of the Yellow River Basin, Quaternary International, 336, 65-72, 10.1016/j.quaint.2013.08.051, 2014.

Wang, J., Gao, H., Liu, M., Ding, Y., Wang, Y., Zhao, F., and Xia, J.: Parameter regionalization of the FLEX-Global hydrological model, Science China Earth Sciences, 1-18, 10.1007/s11430-020-9706-3, 2021.

Wang, Q., Pagano, T., Zhou, S., Hapuarachchi, H., Zhang, L., and Robertson, D.: Monthly versus daily

https://doi.org/10.5194/essd-2022-217
Preprint. Discussion started: 8 September 2022

599 water balance models in simulating monthly runoff, Journal of Hydrology, 404, 166-175,
600 10.1016/j.jhydrol.2011.04.027, 2011.
601 Xia, J., O'Connor, K., Kachroo, R., and Liang, G.: A non-linear perturbation model considering
602 catchment wetness and its application in river flow forecasting, Journal of Hydrology, 200, 164-178,
603 10.1016/S0022-1694(97)00013-9, 1997.
604 Xie, K.: Global soil moisture storage capacity at 0.5° resolution for geoscientific modelling [dataset],
605 10.5281/zenodo.5598405, 2021.
606 Xie, K., Liu, P., Zhang, J., Han, D., Wang, G., and Shen, C.: Physics-guided deep learning for
607 rainfall-runoff modeling by considering extreme events and monotonic relationships, Journal of
608 Hydrology, 603, 10.1016/j.jhydrol.2021.127043, 2021.
609 Xie, K., Liu, P., Zhang, J., Wang, G., Zhang, X., and Zhou, L.: Identification of spatially distributed
610 parameters of hydrological models using the dimension-adaptive key grid calibration strategy -
611 ScienceDirect, Journal of Hydrology, 598, 10.1016/j.jhydrol.2020.125772, 2020a.
612 Xie, K., Liu, P., Zhang, J., Libera, D. A., Wang, G., Li, Z., and Wang, D.: Verification of a New Spatial
613 Distribution Function of Soil Water Storage Capacity Using Conceptual and SWAT Models, Journal of
614 Hydrologic Engineering, 25, 10.1061/(asce)he.1943-5584.0001887, 2020b.
615 Xiong, M., Liu, P., Cheng, L., Deng, C., Gui, Z., Zhang, X., and Liu, Y.: Identifying time-varying
616 hydrological model parameters to improve simulation efficiency by the ensemble Kalman filter: A joint
617 assimilation of streamflow and actual evapotranspiration, Journal of Hydrology, 568, 758-768,
618 10.1016/j.jhydrol.2018.11.038, 2019.
619 Yang, Y., Donohue, R. J., and McVicar, T. R.: Global estimation of effective plant rooting depth:
620 Implications for hydrological modeling, Water Resources Research, 52, 8260-8276,
621 10.1002/2016WR019392, 2016.
622 Zhang, L., Potter, N., Hickel, K., Zhang, Y., and Shao, Q.: Water balance modeling over variable time
623 scales based on the Budyko framework–Model development and testing, Journal of Hydrology, 360,
624 117-131, 10.1016/j.jhydrol.2008.07.021, 2008.
625 Zhang, X. and Liu, P.: A time-varying parameter estimation approach using split-sample calibration
626 based on dynamic programming, Hydrology and Earth System Sciences, 25, 711-733,
627 10.5194/hess-25-711-2021, 2021.
628 Zhang, X., Liu, P., Cheng, L., Liu, Z., and Zhao, Y.: A back-fitting algorithm to improve real-time flood
629 forecasting, Journal of Hydrology, 562, 140-150, 10.1016/j.jhydrol.2018.04.051, 2018.
630 Zhao, R.-J.: The Xinanjiang model applied in China, Journal of hydrology, 135, 371-381, 1992.
631 Zhuo, J.-Y. and Tan, Z.-M.: Physics-Augmented Deep Learning to Improve Tropical Cyclone Intensity
632 and Size Estimation from Satellite Imagery, Monthly Weather Review, 149, 2097-2113,
633 10.1175/MWR-D-20-0333.1, 2021.
634

https://doi.org/10.5194/essd-2022-217
Preprint. Discussion started: 8 September 2022

635 **List of tables**

636 **Table 1.** Research data and sources.

637 **Table 2.** Conceptual parameters to be calibrated in hydrological models.

638 **Table 3.** Results of construction model of global soil moisture storage capacity (SMSC) parameters.

639 **Table 4.** Validation of global SMSC parameters in typical catchments.

640

https://doi.org/10.5194/essd-2022-217
Preprint. Discussion started: 8 September 2022

641

Table 1. Research data and sources.

Data type	Data	Spatial resolution	Time span	Data/product sources
Meteorology	Precipitation Potential evaporation Near-surface temperature	0.5 degree	January 1901 - December 2018 (monthly)	Cru TS 4.03 monthly high-resolution grid data https://data.ceda.ac.uk/badc/cru/data/cru_ts/cru_ts_4.03
Soil and vegetation	Soil thickness			Global 1km grid soil, weathering layer, and sedimentary layer thickness published by ORNL in 2016 https://daac.ornl.gov/SOILS/guides/Global_Soil_Regolith_Sediment.html
	Root zone depth	0.5 degree	/	Global root zone depth products released by Stockholm university in 2016 http://dx.doi.org/10.5194/hess-20-1459-2016-supplement
	Soil type			Upper and lower global soil type data released by USDA https://www.nrcs.usda.gov/wps/portal/nrcs/detail/soils/use/
	Types of land use			AVHRR land-use types issued by NOAA
Topography	Slope Altitude Composite terrain index CTI	0.5 degree	/	GMT global 0.5-degree terrain data released by ISLSCP in 2010 https://daac.ornl.gov/cgi-bin/dsviewer.pl?ds_id=1007
Runoff characteristic	Average flow Runoff coefficient Baseflow coefficient 1% flood discharge	0.5 degree	/	GSCD global runoff data set released by GloH2O in 2015 http://www.gloh2o.org/gscd/
Runoff	Runoff of catchment stations	/	January 1991 - December 2010 (monthly)	GRDC global runoff data center (Including data from more than 10000 stations around the world) https://www.bafg.de/GRDC/EN/Home/homepage_node.html
	Grid runoff	0.5 degree	January 1902 - December 2014 (monthly)	GRUN global grid runoff depth database released by the Federal Institute of technology https://doi.org/10.6084/m9.figshare.9228176

642

https://doi.org/10.5194/essd-2022-217
Preprint. Discussion started: 8 September 2022

643

Table 2. Conceptual parameters to be calibrated in hydrological models.

Model	Parameter	Physical meaning	Minimum boundary	Maximum boundary
DWBM	$SMSC$	Soil moisture storage capacity (mm)	0	1000
	α_1	Retardation coefficient	1	5
	α_2	Evaporation coefficient	1	5
	K_g	Underground runoff coefficient	0.01	1
SWBM	$SMSC$	Soil moisture storage capacity (mm)	0	1000
	K_s	Surface runoff coefficient	0.1	1
	K_g	Underground runoff coefficient	0.01	1
TVGM	$SMSC$	Soil moisture storage capacity (mm)	0	1000
	g_1	Runoff coefficient after soil saturation	0.02	1.0
	g_2	Soil moisture influence coefficient	1.0	5
	K_r	Soil moisture outflow coefficient	0.005	1
	γ	Evaporation conversion index	0.1	1

644

https://doi.org/10.5194/essd-2022-217
Preprint. Discussion started: 8 September 2022

645 **Table 3. Results of construction model of global soil moisture storage capacity (SMSC) parameters.**

Image window	Time interval	Loss function	Evaluating indicator	
		MSE	MAE	R^2
5×5	Training set	0.0032	0.0411	0.8932
	Test set	0.0170	0.0666	0.5935
10×10	Training set	0.0021	0.0341	0.9139
	Test set	0.0061	0.0510	0.7597

646

https://doi.org/10.5194/essd-2022-217
Preprint. Discussion started: 8 September 2022

Open Access Earth System Science Data Discussions

647 **Table 4. Validation of global SMSC parameters in typical catchments.**

Number	Site name	Longitude	Latitude	Drainage area (km^2)	River	KGE (%) of DWBM model		KGE (%) of SWBM model		KGE (%) of TVGM model		Basin average SMSC (mm)
						Cal[1]	Val[2]	Cal	Val	Cal	Val	
1196551	Beibrug	29.99	−22.23	201001	Limpopo	47.06	74.15	53.25	69.67	43.11	41.67	149.84
2181500	Zhimenda	96.6	33.43	137704	Tongtian	49.54	72.26	69.95	77.82	84.71	80.09	121.48
2181900	Datong	117.62	30.77	1705383	Yangtze	55.87	84.52	86.48	91.88	85.75	91.16	206.85
2260500	Sagaing	96.1	21.98	117900	Irrawaddy	78.27	76.35	70.93	68.64	63.22	56.99	365.65
2694450	Waegwan	128.39	36	11195	Naktong	67.81	58.89	66.63	41.78	77.99	44.93	231.37
3268270	Caimancito	−64.47	−23.73	25800	San Francisco	67.54	78.11	53.66	83.31	63.44	63.55	228.89
3618090	Cucui	−66.85	1.22	61781	Negro	69.13	72.83	69.54	67.53	89.36	89.72	226.27
3624120	Gaviao	−66.85	−4.84	162000	Jurua	49.13	66.07	71.06	69.88	88.35	80.24	532.84
3627030	Manicore	−61.30	−5.82	1126700	Madeira	87.15	71.24	68.83	72.46	73.24	86.55	370.19
3629000	Obidos-Porto	−55.51	−1.95	4640300	Amazonas	73.55	80.47	58.66	58.92	57.02	54.63	388.80
3629150	Fortaleza	−57.64	−6.05	358657	Tapajos	39.03	49.10	87.55	74.90	75.24	63.62	428.36
3650745	Ico	−38.87	−6.41	12000	Salgado	39.22	46.87	54.93	63.24	58.56	94.82	392.60
4103800	Eagle AK	−141.20	64.79	293965	Yukon	70.56	77.55	36.05	46.80	37.01	38.99	95.21
4115100	Salem, OR	−123.04	44.94	18855	Willamette	86.86	89.73	80.01	86.28	59.46	66.52	475.76
4115201	Beaver, OR	−123.18	46.18	665371	Columbia	58.60	47.52	79.14	76.35	88.81	74.00	358.43
4119100	Paul, MN	−93.11	44.93	95312	Mississippi	22.95	14.15	60.29	23.76	60.88	55.06	186.30
4146281	Verona, CA	−121.60	38.77	55040	Sacramento	43.65	64.24	70.63	60.40	89.41	88.84	344.22
5109170	Rockfields	142.88	−18.20	10987	Gilbert	52.02	76.95	13.20	50.34	73.34	52.15	245.60
6335180	Worms	8.38	49.64	68827	Rhine	73.97	76.66	78.43	84.00	76.88	78.37	296.07
6342800	Hofkirchen	13.12	48.68	47496	Danube	56.53	46.58	61.31	53.67	69.49	61.30	247.41
Mean KGE						59.42	66.21	64.53	66.08	70.76	68.16	——

648 [1] Calibration period

649 [2] Validation period

https://doi.org/10.5194/essd-2022-217
Preprint. Discussion started: 8 September 2022

List of figures

Figure 1. Structure of depth residual image recognition in convolutional neural network (CNN) model. (a) The spatial distribution of soil moisture storage capacity (SMSC) parameters is obtained by the Shuffled Complex Evolution (SCE-UA) algorithm for the joint calibration. (b) the relationship between the input factors and the regression SMSC parameters is learned by a deep residual network (ResNet). (c) the SMSC parameter dataset is spatially constructed based on the pre-trained ResNet on the grid-scale to fill in data empty areas.

Figure 2. Spatial distribution of labels and construction results for global soil moisture storage capacity (SMSC) parameters. (a) The spatial distribution of the label for deep learning of jointly calibrated SMSC values. (b) The spatial distribution of the constructed global SMSC parameters. (c) The probability density distribution of SMSC parameters calibrated in the labeling area. (e) The probability density distribution of constructed global SMSC parameters. (d) and (f) The distribution of variations of global SMSC with latitude and longitude.

Figure 3. Spatial distribution of other parameter datasets and the differences with global soil moisture storage capacity (SMSC) parameters. (a) The spatial distribution of root zone storage capacity at 0.5° resolution by Wang-Erlandsson et al. (2016). (c) The spatial distribution of rooting depth at 0.5° resolution by Schenk et al. (2009). (b) and (d) The differences between global SMSC parameters and other parameter datasets.

Figure 4. Global distribution of Kling-Gupta efficiency (KGE) simulated by GRUN runoff depth on grid-scale for three monthly water balance models. (a)The KGE of Dynamic Water Balance Model (DWBM). (b) The KGE of Snowbelt-based Water Balance Model (SWBM). (c) The KGE of Time-variant Gain Model (TVGM). (d) The probability density distributions of KGE for three models. (e) The cumulative density distributions of KGE for three models. (f) The boxplot of KGE for three models.

Figure 5. Monthly observed streamflow versus simulated streamflow for three monthly water balance models in typical catchments. Blue dots represent Dynamic Water Balance Model (DWBM). Green dots represent Snowbelt-based Water Balance Model (SWBM). Orange dots represent Time-variant Gain Model (TVGM).

Figure 6. Comparison of constructed SMSC parameter and root zone depth in runoff simulation for three monthly water balance models. The left figure represents the simulation accuracy during recalibration period. The right figure represents the simulation accuracy during validation period. The dots mean the average

https://doi.org/10.5194/essd-2022-217
Preprint. Discussion started: 8 September 2022

677 values, and the lines mean the median values.

678 Figure 7. Spatial correlation between SMSC and input variables by the permutation importance
679 measure. Weights of permutation importance estimate represent the spatial correlation. The larger the
680 absolute value means the more relevant variables.

681

https://doi.org/10.5194/essd-2022-217
Preprint. Discussion started: 8 September 2022

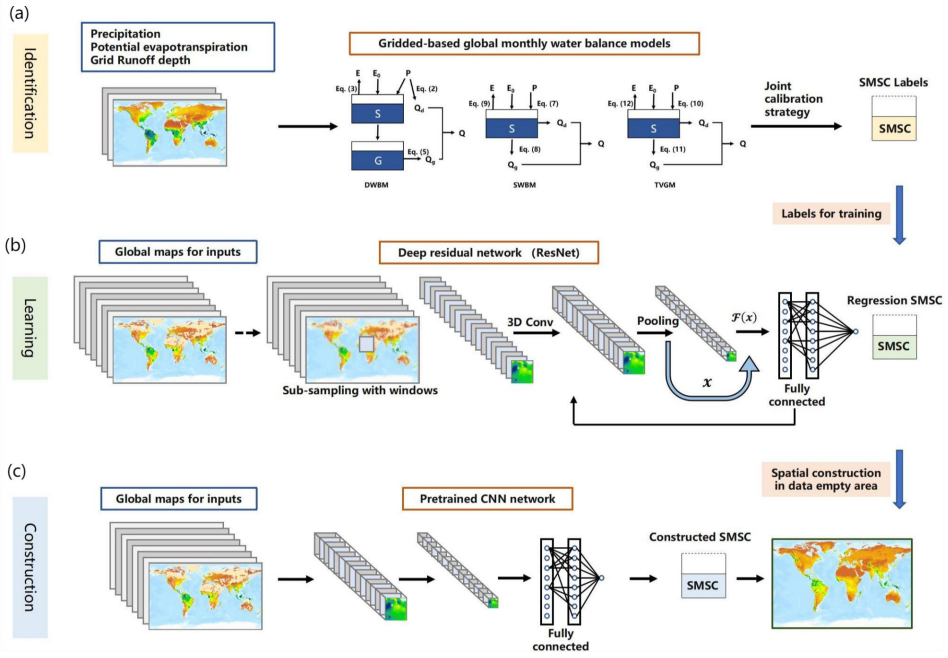

Figure 1. Structure of depth residual image recognition in convolutional neural network (CNN) model. (a) The spatial distribution of soil moisture storage capacity (SMSC) parameters is obtained by the Shuffled Complex Evolution (SCE-UA) algorithm for the joint calibration. (b) the relationship between the input factors and the regression SMSC parameters is learned by a deep residual network (ResNet). (c) the SMSC parameter dataset is spatially constructed based on the pre-trained ResNet on the grid-scale to fill in data empty areas.

https://doi.org/10.5194/essd-2022-217
Preprint. Discussion started: 8 September 2022

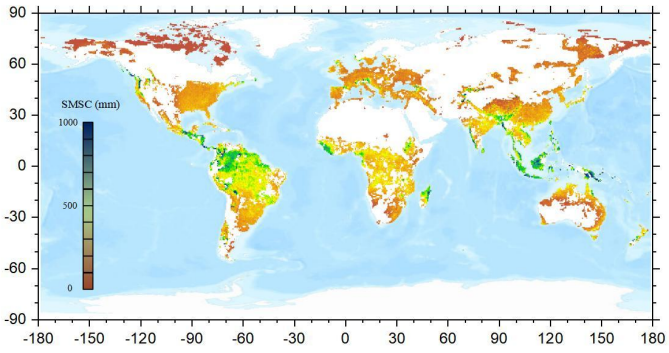

(a) Label for SMSC

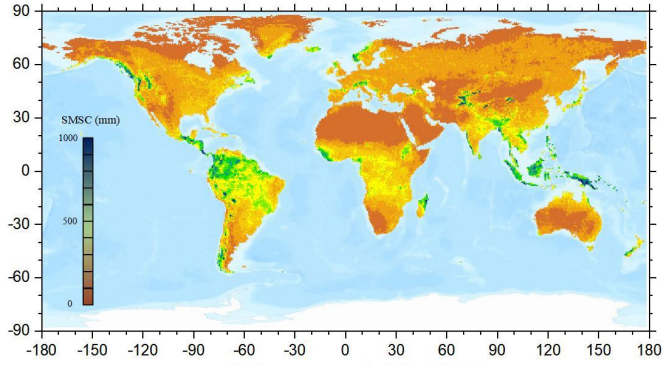

(b) Reconstructed global SMSC

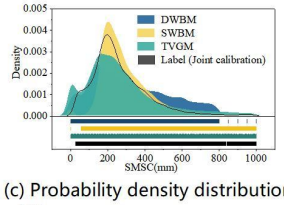

(c) Probability density distribution

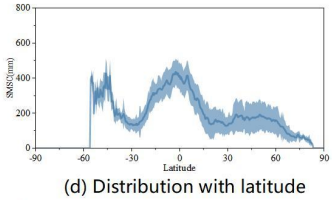

(d) Distribution with latitude

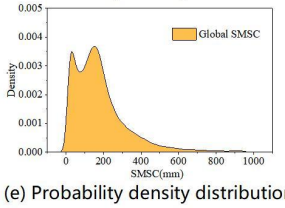

(e) Probability density distribution

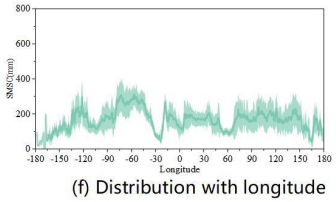

(f) Distribution with longitude

689

690 **Figure 2. Spatial distribution of labels and construction results for global soil moisture storage capacity**
691 **(SMSC) parameters. (a) The spatial distribution of the label for deep learning of jointly calibrated SMSC**
692 **values. (b) The spatial distribution of the constructed global SMSC parameters. (c) The probability density**
693 **distribution of SMSC parameters calibrated in the labeling area. (e) The probability density distribution of**
694 **constructed global SMSC parameters. (d) and (f) The distribution of variations of global SMSC with**
695 **latitude and longitude.**

https://doi.org/10.5194/essd-2022-217
Preprint. Discussion started: 8 September 2022

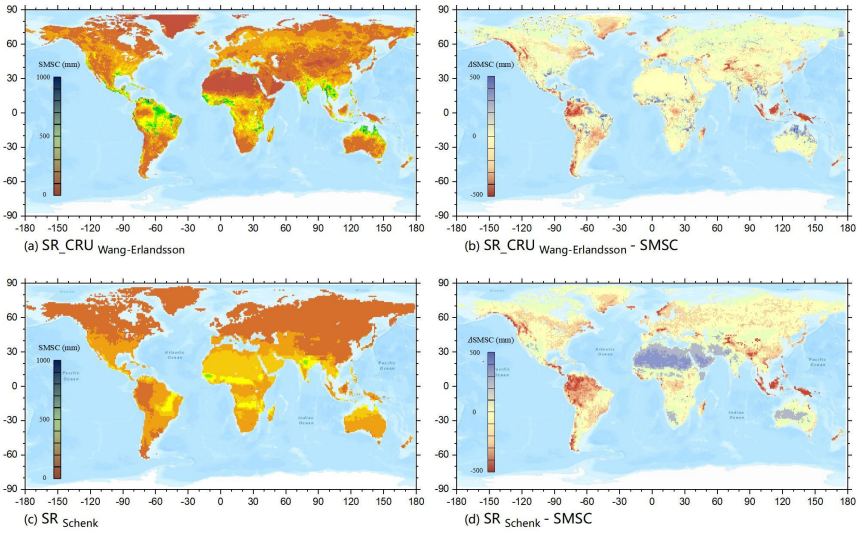

696

697 **Figure 3. Spatial distribution of other parameter datasets and the differences with global soil moisture**
698 **storage capacity (SMSC) parameters. (a) The spatial distribution of root zone storage capacity at 0.5°**
699 **resolution by Wang-Erlandsson et al. (2016). (c) The spatial distribution of rooting depth at 0.5° resolution**
700 **by Schenk et al. (2009). (b) and (d) The differences between global SMSC parameters and other parameter**
701 **datasets.**

https://doi.org/10.5194/essd-2022-217
Preprint. Discussion started: 8 September 2022

Open Access Earth System Science Data Discussions

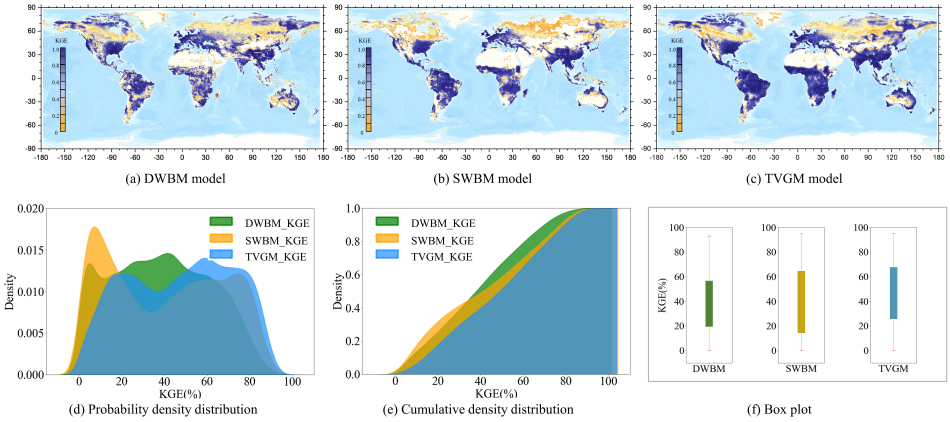

Figure 4. Global distribution of Kling-Gupta efficiency (KGE) simulated by GRUN runoff depth on grid-scale for three monthly water balance models. (a)The KGE of Dynamic Water Balance Model (DWBM). (b) The KGE of Snowbelt-based Water Balance Model (SWBM). (c) The KGE of Time-variant Gain Model (TVGM). (d) The probability density distributions of KGE for three models. (e) The cumulative density distributions of KGE for three models. (f) The boxplot of KGE for three models.

https://doi.org/10.5194/essd-2022-217
Preprint. Discussion started: 8 September 2022

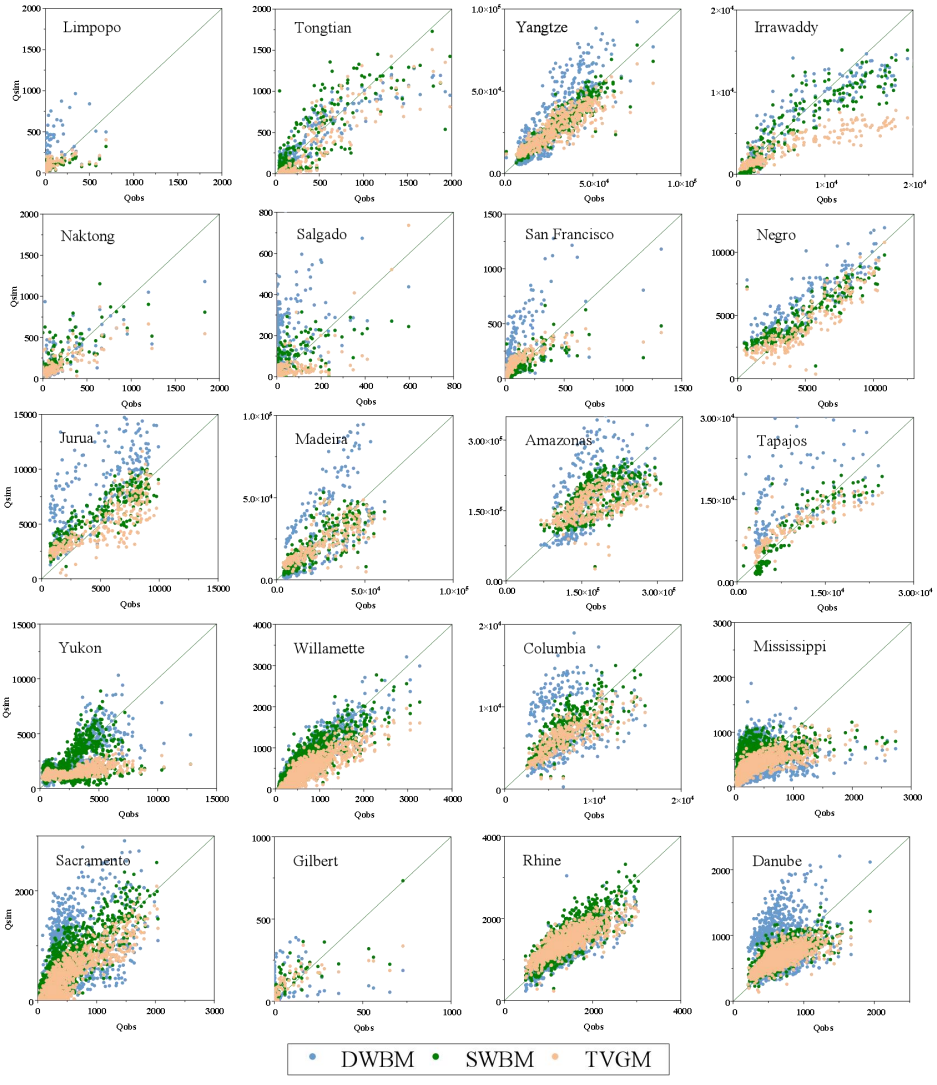

Figure 5. Monthly observed streamflow versus simulated streamflow for three monthly water balance models in typical catchments. Blue dots represent Dynamic Water Balance Model (DWBM). Green dots represent Snowbelt-based Water Balance Model (SWBM). Orange dots represent Time-variant Gain Model (TVGM).

https://doi.org/10.5194/essd-2022-217
Preprint. Discussion started: 8 September 2022

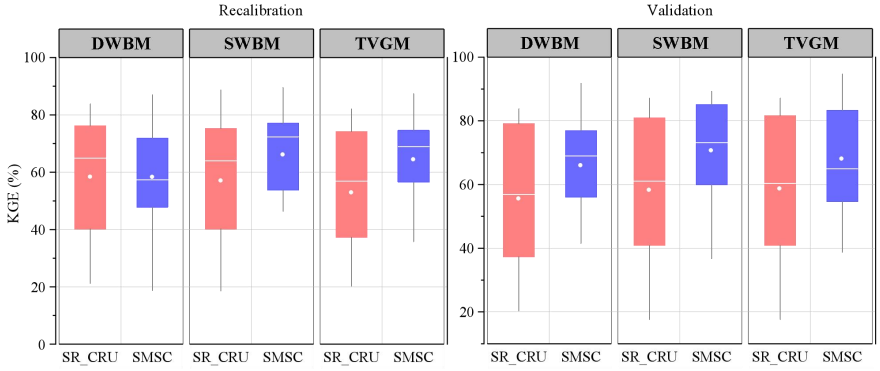

Figure 6. Comparison of constructed SMSC parameter and root zone depth in runoff simulation for three monthly water balance models. The left figure represents the simulation accuracy during recalibration period. The right figure represents the simulation accuracy during validation period. The dots mean the average values, and the lines mean the median values.

https://doi.org/10.5194/essd-2022-217
Preprint. Discussion started: 8 September 2022

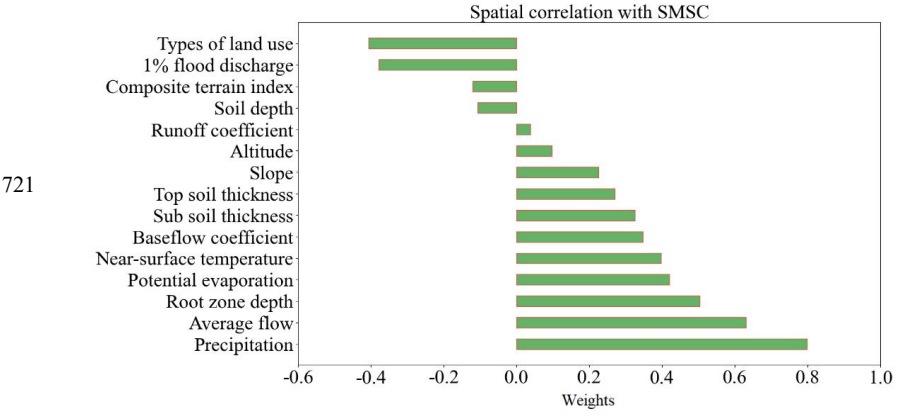

Figure 7. Spatial correlation between SMSC and input variables by the permutation importance measure. Weights of permutation importance estimate represent the spatial correlation. The larger the absolute value means the more relevant variables.